Diffusive behavior in LiMPO$_4$ with M = Fe, Co, Ni probed by muon-spin relaxation

Jun Sugiyama,[1,*] Hiroshi Nozaki,[1] Masashi Harada,[1] Kazuya Kamazawa,[1,†] Yutaka Ikedo,[2] Yasuhiro Miyake,[2] Oren Ofer,[3] Martin Månsson,[4] Eduardo J. Ansaldo,[3] Kim H. Chow,[5] Genki Kobayashi,[6] and Ryoji Kanno[7]

[1]*Toyota Central Research and Development Laboratories Inc., Nagakute, Aichi 480-1192, Japan*

[2]*Muon Science Laboratory, Institute of Materials Structure Science, KEK, 1-1 Oho, Tsukuba, Ibaraki 305-0801, Japan*

[3]*TRIUMF, 4004 Wesbrook Mall, Vancouver, BC, V6T 2A3 Canada*

[4]*Laboratory for Solid State Physics, ETH Zürich, CH-8093 Zürich, Switzerland*

[5]*Department of Physics, University of Alberta, Edmonton, AB, T6G 2G7 Canada*

[6]*Department of Material and Life Chemistry, Faculty of Engineering, Kanagawa University, Yokohama 221-8686, Japan*

[7]*Department of Electronic Chemistry, Interdisciplinary Graduate School of Science and Engineering, Tokyo Institute of Technology, Yokohama 226-8503, Japan*

(Received 23 December 2011; published 14 February 2012)

In order to study the diffusive nature of lithium transition-metal phospho-olivines, we measured muon-spin relaxation (μ^+SR) spectra for the polycrystalline LiMPO$_4$ samples with M = Mn, Fe, Co, or Ni in the temperature range between 50 and 500 K. The μ^+SR spectra under zero applied field are strongly affected by the magnetic moments of the 3d electrons in the M^{2+} ions so that, for LiMnPO$_4$, it was difficult to detect the relaxation change caused by the diffusion due to the large Mn^{2+}($S = 5/2$) moments. However, diffusive behavior was clearly observed via the relaxation due to nuclear dipolar fields above ~150 K for LiFePO$_4$, LiCoPO$_4$, and LiNiPO$_4$ as S decreased from 2 to 1. From the temperature dependence of the nuclear field fluctuation rate, self-diffusion coefficients of Li$^+$ ions (D_{Li}) at 300 K and its activation energy (E_a) were estimated, respectively, as ~3.6(2) × 10^{-10} cm^2/s and E_a = 0.10(2) eV for LiFePO$_4$, ~1.6(1) × 10^{-10} cm^2/s and E_a = 0.10(1) eV for LiCoPO$_4$, and ~2.7(4) × 10^{-10} cm^2/s and E_a = 0.17(2) eV for LiNiPO$_4$, assuming that the diffusing Li$^+$ ions jump between the regular site and interstitial sites.

DOI: 10.1103/PhysRevB.85.054111 PACS number(s): 76.75.+i, 66.30.H−, 82.47.Aa, 82.56.Lz

I. INTRODUCTION

Among several methods to detect self-diffusion of Li$^+$ ions in solids, the muon-spin relaxation (μ^+SR) technique provides unique information on Li diffusion, mainly because of its characteristic time and spatial resolutions.[1] Furthermore, when using muons with momentum p_μ = 29.8 MeV/c and kinetic energy K_μ = 4.1 MeV—that is, *surface muons*—the initial muon-spin direction is perfectly antiparallel to its momentum. This is a significant advantage over NMR and other resonance techniques, since such 100% *spin-polarized* muons sense the internal magnetic field under zero applied field (ZF). As a result, even when the muon spins are depolarized by internal fields of both electronic and nuclear origin,[2] as in materials containing magnetic ions, the electronic contribution is, in principle, distinguishable from the nuclear contribution by longitudinal field (LF, parallel to the initial muon spin) measurements.[3]

In fact, μ^+SR gave a more reliable self-diffusion coefficient for Li$^+$ ions (D_{Li}) than Li-NMR[4] in Li$_x$CoO$_2$, well known as a common cathode material for Li-ion batteries.[5] This is because the magnetic ions contribute additional spin-lattice relaxation processes with considerably greater $1/T_1$ fs than expected from only Li diffusion.[6,7] As a result, D_{Li} estimated by ^{7}Li-NMR for LiCoO$_2$ and LiNiO$_2$[8] is three or four orders of magnitude smaller than the D_{Li} predicted by first principles calculations,[9] while μ^+SR yields higher D_{Li} for the related compounds LiNiO$_2$ and LiCrO$_2$, more in line with the theoretical predictions.[10]

Very recent μ^+SR work on the olivine-type lithium iron phosphate LiFePO$_4$, which is heavily investigated as a positive electrode material for the near-future Li-ion battery,[11,12] showed that $D_{\mathrm{Li}} \sim 3.6 \times 10^{-10}$ cm^2/s at 300 K,[13] a result confirmed by another group.[14] Regarding the reliability of the estimation, the D_{Li} value obtained by μ^+SR is consistent with recent electrochemical simulations using the chronoamperometric response data, in which $D_{\mathrm{Li}} \sim 7.6 \times 10^{-11}$ cm^2/s for Li$_{0.999}$FePO$_4$ at ambient temperature (T),[15] while first-principles calculations predicted $D_{\mathrm{Li}} \sim 10^{-8}$cm^2/s for the Li$_{7/8}$FePO$_4$ case.[16] In contrast to D_{Li}, the chemical diffusion coefficient ($\tilde{D}_{\mathrm{Li}}$), which is measured under a potential gradient, is reported to range between 4.06×10^{-11} cm^2/s and 5.8×10^{-16} cm^2/s,[17–21] depending on the measurement technique, morphology of LiFePO$_4$ particles or electrode, and electrolyte. It is, therefore, highly desirable to obtain reliable estimates of the intrinsic D_{Li} of positive electrode materials by μ^+SR.

The other lithium transition-metal phospho-olivines; namely, LiMPO$_4$ with M = Mn, Co, or Ni are also regarded as potentially useful positive electrode materials,[22] since they are more stable than layered transition-metal dioxides, LiMO$_2$ with M = Mn, Co, or Ni, at moderately high T. In fact, since the theoretical energy density of LiMnPO$_4$ is higher than that of LiFePO$_4$, a solid solution between LiFePO$_4$ and LiMnPO$_4$ has been investigated as a candidate system for overcoming the slow electrochemical response of LiMnPO$_4$.[23,24] However, there is, to our knowledge, no systematic electrochemical work on LiMPO$_4$ from M = Mn to Ni through Fe and Co, although their magnetic nature has been extensively investigated by several techniques,[25–35] including our μ^+SR work at low T.[13,36] In particular, all four compounds exhibit a magnetic transition from a Curie-Weiss paramagnetic phase to an antiferromagnetic (AF) ordered phase at T_{N} = 23 to 53 K.

From the μ^+SR viewpoint, with the goal of determining $D_{\rm Li}$ in Curie-Weiss paramagnets, the LiMPO$_4$ system is expected to provide interesting insights concerning the competition between fields of electronic and nuclear origin. This is because the number of $3d$ electrons of the M^{2+} ions systematically increases from 5 ($S = 5/2$) to 8 ($S = 1$) from Mn to Ni in a distorted MO_6 octahedron in the olivine lattice. In other words, we could disentangle the effect of localized $3d$ moments on the nuclear induced relaxation in the μ^+SR spectrum by a systematic study on LiMPO$_4$. Following upon the work on LiFePO$_4$, we have, therefore, investigated the microscopic magnetic nature of LiMPO$_4$ by μ^+SR, particularly for clarifying the diffusive behavior in their paramagnetic state. Here, we report the results for Li diffusion in LiMnPO$_4$, LiCoPO$_4$, and LiNiPO$_4$, combined with the previous data for LiFePO$_4$.

II. EXPERIMENTAL

Powder samples of LiMPO$_4$ were prepared by a solid-state-reaction technique using reagent grade Li_2CO_3, Mn(II)C_2O_4∗0.5H_2O, Fe(II)C_2O_4∗2H_2O, Co(II)C_2O_4, Ni(II)C_2O_4∗2H_2O, and $(NH_4)_2HPO_4$ as starting materials. A stoichiometric mixture of the raw materials was thoroughly mixed by a conventional planetary milling apparatus, and then, the mixture was sintered at 700 °C for 6 h in a purified argon-gas flow for LiMnPO$_4$ and LiFePO$_4$, but at 750 °C for 6 h in a purified argon gas flow for LiCoPO$_4$ and LiNiPO$_4$. According to powder x-ray diffraction (XRD) analysis, the samples were a single phase of orthorhombic symmetry with space group $Pnma$. In order to know the macroscopic magnetic properties of the sample, the susceptibility χ was measured below 400 K under a $H \leqslant 10$ kOe field with a superconducting quantum interference device (SQUID) magnetometer (MPMS, Quatum Design). The Weiss temperature ($\Theta_{\rm CW}$) and effective magnetic moment ($\mu_{\rm eff}$) were determined from the $\chi(T)$ curve by fitting to a Curie-Weiss law, $\chi = C/(T - \Theta_{\rm CW})$ with $C = [Ng^2\mu_{\rm B}^2/(3k_{\rm B})]\mu_{\rm eff}^2$ in the T range between 100 and 400 K, as seen in Fig. 1. Here, N is the number density of M spins, g is the Landé g factor, $\mu_{\rm B}$ is the Bohr magneton, and $k_{\rm B}$ is Boltzmann's constant. The results for the four samples are summarized in Table I. These values are consistent with those from the literature.[22,23,25,26]

The μ^+SR spectra were mainly measured at the surface muon beamlines using the D-OMEGA1 spectrometer of the Muon Science Establishment (MUSE) of the Materials and Life Science Experimental Facility (MLF) at the Japan Proton Accelerator Research Complex (J-PARC) in Japan. Typically, a ∼2 g powder sample was pressed into a disk with 27 mm diameter and 1 mm thickness and packed into a Au O-ring-sealed titanium cell. The window of the cell was made of a Kapton film with 50 μm thickness. The cell was mounted onto the Cu plate of a liquid-He-flow–type cryostat for measurements between 100 and 500 K. In order to get information in the early time domain, additional μ^+SR measurements were performed using the Los Alamos Meson Physics Facility (LAMPF) spectrometer of the M20 beamline at the Tri-University Meson Facility (TRIUMF) in Canada, for which the approximately 500 mg powder sample was placed in an envelope with 1 × 1 cm^2 area, made with Al-coated Mylar tape with 0.05 mm thickness in order to minimize the signal from the envelope. Then, the envelope was attached to a low-background sample holder in a liquid-He-flow–type cryostat for measurements in the T range between 50 and 150 K. The experimental techniques are described in more detail elsewhere.[1]

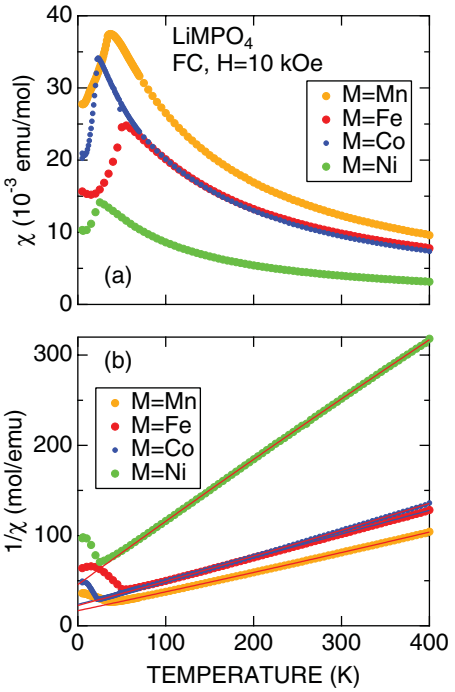

FIG. 1. (Color online) T dependence of (a) susceptibility χ and (b) $1/\chi$ for LiMPO$_4$. The χ data were obtained in field-cooling (FC) mode with $H = 10$ kOe. In (b), solid lines represent a linear fit in the T range between 100 and 400 K using the Curie-Weiss formula.

III. RESULTS

In order to understand the overall variation of the μ^+SR spectrum with T, Fig. 2 shows representative ZF and LF spectra for LiMPO$_4$ with M = Fe, Co, or Ni obtained at 100, 300, and 480 K. At each T, the ZF spectrum of LiFePO$_4$ and LiCoPO$_4$ consists of a fast relaxing signal in the early-time domain and a slowly relaxing signal. The former is caused by a fluctuating magnetic field ($H_{\rm int}^{3d}$) due to the $3d$ electrons of the M^{2+} ions, while the latter is caused by nuclear magnetic fields ($H_{\rm int}^{\rm N}$) due to ^{6}Li, ^{7}Li, ^{57}Fe, ^{59}Co, ^{61}Ni, and ^{31}P. Since the natural abundance of ^{57}Fe, ^{59}Co, and ^{61}Ni is 2.2%, 100%, and 1.14%, respectively, the effect of ^{57}Fe and ^{61}Ni on $H_{\rm int}^{\rm N}$ is negligible small. Note that the ZF spectrum of LiNiPO$_4$

TABLE I. The Weiss temperature $\Theta_{\rm CW}$, effective magnetic moment $\mu_{\rm eff}$, and Néel temperature $T_{\rm N}$ for the four LiMPO$_4$ samples. Here, we assumed $g = 2$ for the $\mu_{\rm eff}$ estimation.

M	$\Theta_{\rm CW}$ (K)	$\mu_{\rm eff}$ ($\mu_{\rm B}$)	$T_{\rm N}$ (K)
Mn	−68.6(5)	6.02 (1)	37 (1)
Fe	−89.4(2)	5.53 (1)	53 (1)
Co	−69.0(6)	5.27 (1)	25.0 (5)
Ni	−74.4(4)	3.45 (1)	23.0 (5)

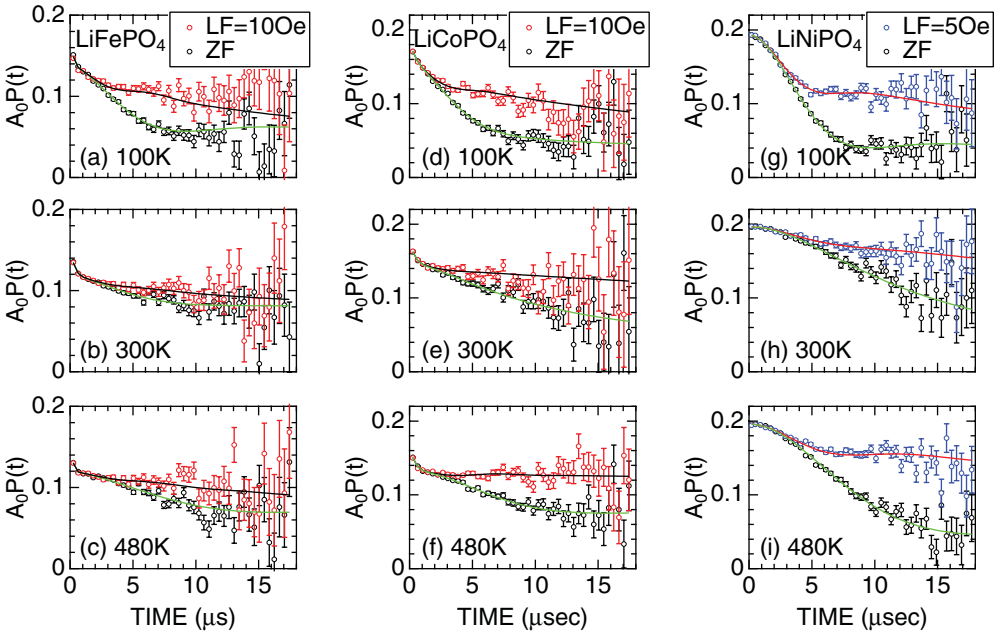

FIG. 2. (Color online) ZF and LF μ^+SR spectra for LiFePO$_4$, LiCoPO$_4$, and LiNiPO$_4$ obtained at (a) [(d),(g)] 100 K, (b) [(e),(h)] 300 K, and (c) [(f),(i)] 480 K. The applied LF was 10 Oe for LiFePO$_4$ and LiCoPO$_4$ and 5 Oe for LiNiPO$_4$. Solid lines represent the fit result using Eq. (1). These spectra were obtained at J-PARC.

shows a typical Kubo Toyabe behavior and lacks a fast-relaxing component.

The applied LF (=10 Oe or 5 Oe) clearly reduces the relaxation rate of the slowly relaxing signal (i.e., decouples $H_{\rm int}^{\rm N}$, at 100 K). However, such a "decoupling" effect is very weak at 300 K even for LiNiPO$_4$, indicating the increase in fluctuation rate of $H_{\rm int}^{\rm N}$ (ν) with T. Interestingly, the same LF reduces the relaxation rate again at 480 K, which means that $H_{\rm int}^{\rm N}$ shows a static nature at 100 K, but dynamic at 300 K and then becomes static like again at 480 K.

In contrast to LiMPO$_4$ with M = Fe, Co, or Ni, the ZF spectrum for LiMnPO$_4$ consists of the tail of a very rapidly relaxing signal and a time-independent offset signal from the Ti cell (Fig. 3), which indicates the presence of a large fluctuating field due to Mn^{2+} ($S = 5/2$) moments even at 300 K for LiMnPO$_4$. As a result, it is very difficult to estimate the field distribution width (Δ) and ν by μ^+SR for this case and,

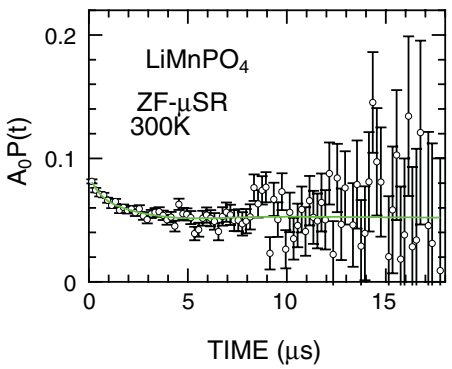

FIG. 3. (Color online) ZF μ^+SR spectrum for LiMnPO$_4$ at 300 K. Solid lines represent the fit result using Eq. (1) with $A_{\rm KT} = 0$. The spectrum was obtained at J-PARC.

therefore, we concentrated further measurements on LiFePO$_4$, LiCoPO$_4$, and LiNiPO$_4$.

In order to know the change in $H_{\rm int}^{3d}$ and $H_{\rm int}^{\rm N}$ with T for LiMPO$_4$ with M = Fe, Co, or Ni, the ZF and LF spectra were fit simultaneously by a combination of an exponentially relaxating signal caused by $H_{\rm int}^{3d}$, an exponentially relaxing dynamic Gaussian Kubo Toyabe (KT) function [$G^{\rm DGKT}(\Delta,\nu,t,H_{\rm LF})$] caused by a fluctuating $H_{\rm int}^{\rm N}$ due respectively to 3d moments and Li diffusion,[2] plus an offset background (BG) signal from the fraction of muons stopped mainly in the sample cell, which is made of high-purity titanium:

$$A_0\,P_{\rm LF}(t) = A_{\rm F}\exp(-\lambda_{\rm F}t) + A_{\rm KT}\exp(-\lambda_{\rm KT}t) \times G^{\rm DGKT}(\Delta,\nu,t,H_{\rm LF}) + A_{\rm BG}, \quad (1)$$

where A_0 is the initial ($t = 0$) asymmetry, $A_{\rm F}$, $A_{\rm KT}$, and $A_{\rm BG}$ are the asymmetries associated with the three signals. $\lambda_{\rm F}$ and $\lambda_{\rm KT}$ are the exponential relaxation rates, Δ is the static width of the local field distribution at the disordered sites, and ν is the field fluctuation rate. When $\nu = 0$ and $H_{\rm LF} = 0$, $G^{\rm DGKT}(t,\Delta,\nu,H_{\rm LF})$ is the static Gaussian KT function $G_{zz}^{\rm KT}(t,\Delta)$ in ZF. Equation (1) suggests the presence of two different muon sites, consistent with the low-T results.[13,36]

Here, the $A_{\rm F}$ signal should be given by $A_{\rm F}G^{\rm DGKT}(\Delta,\nu,t,H_{\rm LF})\exp(-\lambda_{\rm F}t)$, as well as the second term of Eq. (1). However, when $\lambda_{\rm F} \gg \Delta$ or ν, as demonstrated later, $\exp(-\lambda_{\rm F}t)$ is predominant for the $A_{\rm F}$ signal. Thus, we used $A_{\rm F}\exp(-\lambda_{\rm F}t)$ instead. For LiNiPO$_4$, due to the absence of a fast relaxing signal in the early time domain [see Figs. 2(g)–2(i)], the spectra were fit by Eq. (1) with $A_{\rm F} = 0$.

At first, we fit all the ZF and LF spectra using a common $A_{\rm BG}$ in the whole T range and common (i.e., $H_{\rm LF}$ independent) Δ and ν at each T in Eq. (1). Then, since both $\lambda_{\rm F}$ and $\lambda_{\rm KT}$ were found to be approximately T independent (see Appendix),

TABLE II. T-independent μ^+SR parameters for $LiFePO_4$, $LiCoPO_4$, and $LiNiPO_4$. The data were obtained by fitting globally the ZF and LF spectra using Eq. (1). Since the power and tune of the muon beam in J-PARC varied during the experiments, A_{BG} changed with M, despite the use of the same Ti cell for the measurements. The magnitude of A_0 depends on both A_F and λ_F. Here, λ_F is only a rough estimate because the μ^+SR signal cannot be measured at early times below ~200 ns due to the pulsed nature of the beam. More correctly, since the pulse width is 100 ns,[37] the signal is more-or-less distorted until 200 ns.

M	A_{BG}	A_{BG}/A_0	λ_F (10^6 s^{-1})	λ_{KT} (10^6 s^{-1})
Fe	0.052 (1)	0.302[a]	4.1 (2)	0.017 (4)
Co	0.047 (1)	0.244[a]	2.68 (7)	0.004 (2)
Ni	0.033 (1)	0.169	0	0

[a]At 100 K.

we finally used common λ_F and λ_{KT} for fitting the ZF and LF spectra. The values obtained are summarized in Table II. The origin of λ_F and λ_{KT} are naturally the coupling between localized Fe or Co moments and muon-spins. If we assume that the coupling constants J_F and J_{KT} are rather small compared with T, both λ_F and λ_{KT} are thought to be T independent.

Figure 4 shows the T dependencies of μ^+SR parameters for $LiMPO_4$ obtained by such a global fitting. For $LiFePO_4$, as T increases from 100 K, Δ is almost independent of T until ~200 K, and decreases slightly with T, then finally levels off to a constant value (~0.1×10^{-6} s^{-1}) above ~300 K. On the other hand, ν starts to increase above around 150 K ($=T_{start}$)

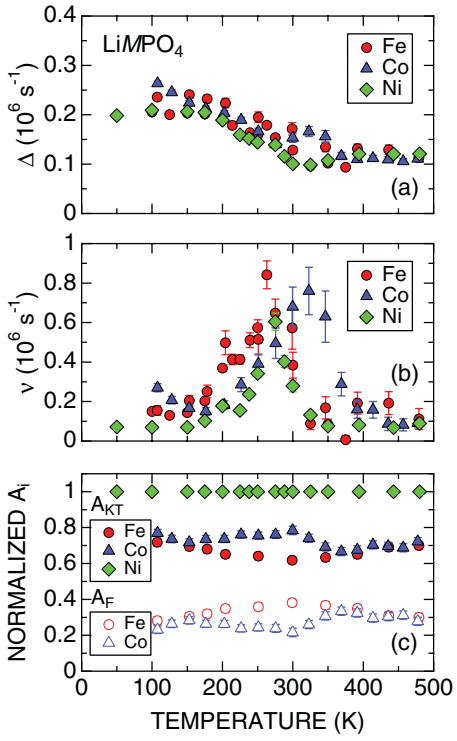

FIG. 4. (Color online) T dependencies of (a) Δ and ν and (b) normalized A_{KT} and A_F [$A_{KT}/(A_{KT}+A_F)$ and $A_F/(A_{KT}+A_F)$] for $LiMPO_4$. Each data point was obtained by global-fitting the ZF and LF spectra using Eq. (1).

with increasing slope ($d\nu/dT$), reaches a maximum at 260 K ($=T_{peak}$), and then decreases with further increasing T. Then, ν also becomes T independent at T above 325 K ($=T_{end}$).

The $\Delta(T)$ and $\nu(T)$ curves for $LiCoPO_4$ and $LiNiPO_4$ are similar to those for $LiFePO_4$, although T_{peak} varies with M. Since all the samples show a static behavior above T_{peak}, the possibility that muons diffuse above T_{peak} is excluded. This is consistent with the results of electrostatic potential calculations for $LiMPO_4$, as shown in Secs. IV A and IV B. Therefore, we conclude that the Li^+ ions start to diffuse above T_{start} and their diffusion rate increases with T. Finally, since ν becomes rather large compared with Δ, such diffusion is too fast to be visible by μ^+SR. As a result, ν decreases with T above T_{peak} and, finally, ν (Δ) corresponds to the nuclear field fluctuation rate (nuclear field distribution width) mainly by ^{58}Co and ^{31}P above T_{end}. The diffusive behavior detected by μ^+SR will be discussed in detail in Sec. IV B.

The two asymmetries are found to vary with T, particularly at around 300 K. This is because, since the Li^+ ions are diffusing, the distribution of electrostatic potential in the lattice is naturally altered by Li^+ diffusion. As a result, the stability of each muon site is thought to depend on T.

IV. DISCUSSION

A. Muon sites

Assuming that each μ is bound to the nearest O^{2-} ion with a typical bond length in oxides, namely, $d_{\mu\text{-}O} = 1$ Å,[1] electrostatic potential (E) calculations using a point charge model suggested that there are four possible muon sites in the vicinity of the O^{2-} ions in the $LiFePO_4$ and $LiCoPO_4$ lattice, as seen in Fig. 5, whereas there are three sites for $LiMnPO_4$ and $LiNiPO_4$ (see Table III). In particular, E shows a local minimum at the μ_{12} position for the four compounds, but due to a slight change in the lattice parameters and atomic positions, a new potential minimum appears at the μ_{11} position only for $LiFePO_4$ and $LiCoPO_4$. However, the E values for μ_{12} and μ_{11} are higher by 0.7 to 1.8 eV than those for μ_{31} and higher by 1.7 to 2.2 eV than those for μ_{21}, indicating that the implanted muons are most unlikely to sit at the μ_{11} and μ_{12} sites. In addition, since the μ_{12} site is too close to the Li diffusive pathway parallel to the b axis,[38,39] such a site is anticipated to be unstable for the muons, particularly when the Li^+ ions start

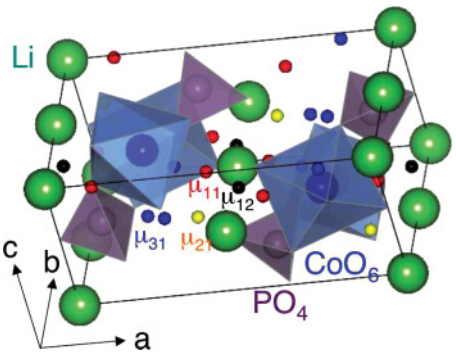

FIG. 5. (Color online) Possible muon sites (μ11, μ12, μ21, and μ31) for $LiCoPO_4$ predicted by electrostatic potential calculations.

TABLE III. Possible muon sites (μ_{nm}), which locate 1 Å away from O$_n$, the distance between μ_{nm} and the nearest M^{2+} ion, electrostatic potential (E) at μ_{nm}, the electronic field distribution width ($\Delta H_{\rm int}^{3d}$), nuclear dipole field distribution width (Δ) for LiMPO$_4$ determined by electrostatic potential calculations and dipole field calculations. $\Delta^{M\rm PO_4}$ is Δ without Li nuclear magnetic moments. The calculations were performed with the DIPELEC program,[46] based on a point charge model.

M	Site	Nearest O site (x,y,z)	(x,y,z)	$d_{\mu-M}$ (Å)	E (eV)	$\Delta H_{\rm int}^{3d}$ (Oe/$\mu_{\rm B}$)	$\Delta H_{\rm int}^{3d}$ ($\times 10^6$ s^{-1} $\mu_{\rm B}^{-1}$)	Δ ($\times 10^6$ s^{-1})	$\Delta^{M\rm PO_4}$ ($\times 10^6$ s^{-1})
Mn	μ12	O1 (0.099,0.250,0.732)	(0.0467,0.2500,0.9090)	2.477	−9.841	614	52.3	0.466	0.138
	μ21	O2 (0.456,0.250,0.216)	(0.3943,0.2500,0.3777)	2.247	−11.526	784	66.7	0.312	0.159
	μ31	O3 (0.157,0.047,0.274)	(0.1687, − 0.0473,0.1031)	2.198	−10.572	1018	86.7	0.310	0.202
Fe	μ11	O1 (0.097,0.250,0.742)	(0.1225,0.3772,0.8679)	1.885	−9.214	1196	101.8	0.372	0.076
	μ12	O1 (0.097,0.250,0.742)	(0.0416,0.2500,0.9172)	2.501	−9.119	611	52.0	0.490	0.076
	μ21	O2 (0.457,0.250,0.206)	(0.3901,0.2500,0.3599)	2.129	−11.176	887	75.6	0.265	0.061
	μ31	O3 (0.166,0.046,0.285)	(0.1858, − 0.0426,0.1106)	2.154	−10.788	1152	98.1	0.199	0.065
Co	μ11	O1 (0.092,0.250,0.745)	(0.1190,0.3853,0.8577)	1.890	−9.005	1265	107.8	0.482	0.317
	μ12	O1 (0.092,0.250,0.745)	(0.0303,0.2500,0.9103)	2.541	−8.862	623	53.1	0.535	0.169
	μ21	O2 (0.450,0.250,0.219)	(0.3831,0.2500,0.3746)	2.153	−11.246	906	77.2	0.347	0.228
	μ31	O3 (0.162,0.045,0.276)	(0.1802, − 0.0493,0.1038)	2.165	−10.807	1167	99.4	0.352	0.155
Ni	μ12	O1 (0.092,0.250,0.745)	(0.0240,0.2500,0.9014)	2.554	−9.678	615	52.3	0.545	0.076
	μ21	O2 (0.450,0.250,0.219)	(0.3872,0.2500,0.3852)	2.195	−11.830	849	72.3	0.293	0.062
	μ31	O3 (0.162,0.045,0.276)	(0.1697, − 0.0570,0.1052)	2.158	−10.657	1109	94.4	0.263	0.067

to diffuse at high T. Therefore, in the following discussion, we assume that the muons locate at the μ_{21} and/or μ_{31} sites.

Now, we discuss the change in the relaxation rate ($\lambda_{\rm F}$) of the fast-relaxing signal with M. Although Tables I and III provide several magnetic parameters including $\mu_{\rm eff}$ and the magnetic field distribution width ($\Delta H_{\int}^{3d}$) due to M^{2+} ions, there is no clear correlation between these parameters and $\lambda_{\rm F}$. However, S of the M^{2+} ions is highly likely to correlate with $\lambda_{\rm F}$ (see Fig. 6). Since the origin of $\lambda_{\rm F}$ is thought to be a direct coupling between the muon-spin and localized M^{2+} spins, as mentioned in Sec. III, S should be the more reasonable parameter for affecting $\lambda_{\rm F}$ than $\mu_{\rm eff}$. This is also an acceptable explanation if we consider the difference of the time window between the μ^+SR and dc-χ measurements. Such a rapid increase in $\lambda_{\rm F}$ at $S > 2$ is also known for several transition-metal oxides. For β''-LiFeO$_2$[40] and α-NaFeO$_2$,[41] in which the Fe^{3+} ions are in a high-spin state with $S = 5/2$, a Kubo-Toyabe behavior is not observed even at 300 K, as is the case for LiMnPO$_4$. On the other hand, for LiMn$_2$O$_4$, in which Mn^{3+} (Mn^{4+}) ions are in an $S = 2$ ($S = 3/2$) state, a clear nuclear relaxation was observed above $T_{\rm N}$.[42–44]

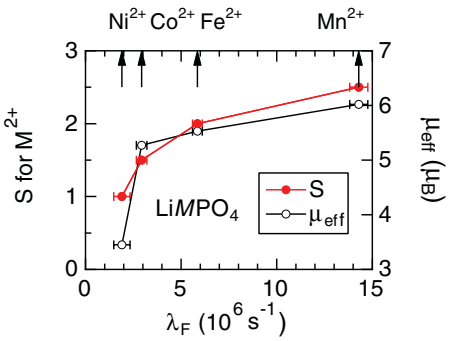

FIG. 6. (Color online) The relationship between (a) the spin quantum number (S) of the M^{2+} ions and $\lambda_{\rm F}$ and (b) the effective magnetic moment ($\mu_{\rm eff}$) and $\lambda_{\rm F}$. $\lambda_{\rm F}$ was obtained by fitting the wTF, ZF, and LF spectra at $T \sim 2T_{\rm N}$ using Eq. (1). In order to better assess the fast relaxation at early times, the spectra were measured at TRIUMF using the same samples that were measured at J-PARC.

B. Li diffusive behavior

In this section, we discuss the evaluation of the self-diffusion coefficients of Li$^+$ ions ($D_{\rm Li}$) from the present μ^+SR results. Since the regular Li site is fully occupied by Li, we naturally consider jumps to interstitial sites. The E calculations suggest two possible interstitial sites for Li diffusion in LiMPO$_4$ with M = Fe, Co, or Ni, as seen in Fig. 7. Although the point charge model provides a rough estimate for the distribution of E even for an insulating material, Fig. 7 is most likely to support that not muons but Li$^+$ ions are diffusing in the lattice. This is because the lowest E in the ab plane, on which the Li$^+$ ions locate, is still higher by 4 to 5 eV than E for the muon sites listed in Table III.

Assuming that ν corresponds to the jump rate of the Li$^+$ ions between the neighboring sites, $D_{\rm Li}$ is given by[47]

$$D_{\rm Li} = \sum_{i=1}^{n} \frac{1}{N_i} Z_{v,i} s_i^2 \nu, \qquad (2)$$

where N_i is the number of Li sites in the ith path, $Z_{v,i}$ is the vacancy fraction, and s_i is the jump distance. Therefore, $n = 2$, $N_1 = 2$, and $Z_1 = 1$ and $N_2 = 2$, and $Z_2 = 1$. From Fig. 7, $s_1 = 1.86$ Å and $s_2 = 1.77$ Å for LiFePO$_4$, $s_1 = 1.84$ Å and $s_2 = 1.80$ Å for LiCoPO$_4$, and $s_1 = 1.69$ Å and $s_2 = 1.66$ Å for LiNiPO$_4$.

In order to extract the contribution of Li diffusion from ν, we fit the ν-vs-$1/T$ curve by a combination of a thermal activation process due to Li diffusion and a T-independent offset signal caused by the fluctuation of M moments [Fig. 8(a)]. That is, $\nu = \nu_0 \exp[-E_a/(k_{\rm B}T)] + \nu_M$, where $E_{\rm a}$ is the activation energy and $k_{\rm B}$ is Boltzmann's constant. Using $(\nu - \nu_M)$ instead of

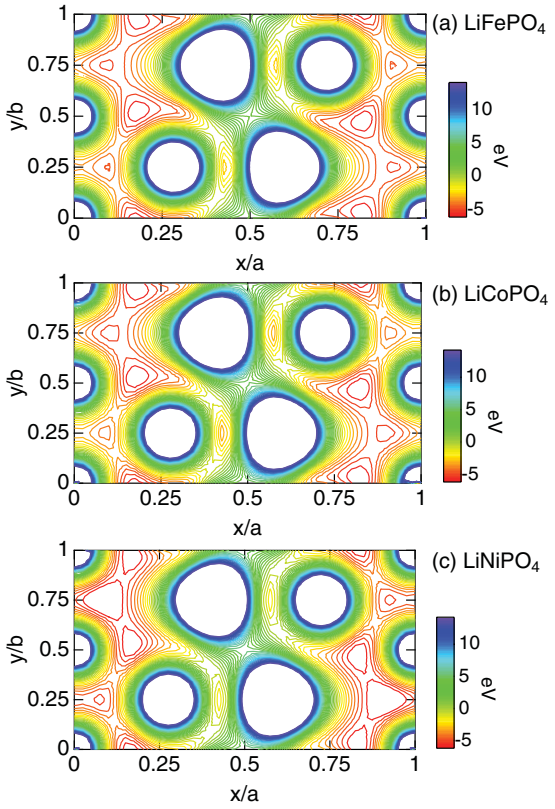

FIG. 7. (Color online) Electrostatic potential distribution in the $(x,y,0)$ plane for (a) $LiFePO_4$, (b) $LiCoPO_4$, and (c) $LiNiPO_4$. There are two potential minima around the regular Li sites, (0, 0, 0) and (0, 0.5, 0). That is, (0.090, 0.748, 0) and (0.180, 0.523, 0) for $LiFePO_4$, (0.100, 0.749, 0) and (0.180, 0.526, 0) for $LiCoPO_4$, and (0.085, 0.751, 0) and (0.165, 0.526, 0) for $LiNiPO_4$. The lattice constants are $a = 10.3377$ Å and $b = 6.0112$ Å for $LiFePO_4$, $a = 10.2011$ Å and $b = 5.9234$ Å for $LiCoPO_4$, and $a = 10.0275$ Å and $b = 5.8537$ Å for $LiNiPO_4$.

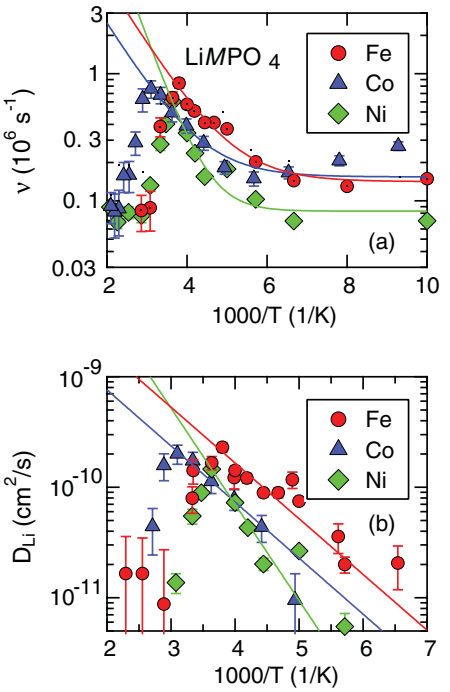

FIG. 8. (Color online) Relationship between D_{Li} and $1/T$. The straight line shows the thermally activated behavior discussed in the text.

ν in Eq. (2), we obtained the T dependence of D_{Li} for $LiMPO_4$ [Fig. 8(b)]. One can clearly see that the slope (E_a) varies with M. Both D_{Li} at 300 K and E_a are summarized in Table IV.

Unfortunately, reliable estimates of D_{Li} are currently unavailable not only for $LiFePO_4$[23] but also $LiMPO_4$ with $M = Mn$, Co, or Ni. Even for $\tilde{D}_{Li}$, there are a very limited number of reports; that is, $\tilde{D}_{Li}$ ranges between 8.8×10^{-15} and 5.056×10^{-14} cm^2/s for $LiMnPO_4$,[48,49] and $\tilde{D}_{Li} \sim 1 \times 10^{-12}$ cm^2/s for $LiCoPO_4$,[50] whereas there is no work reported for $LiNiPO_4$. Therefore, we compare the present μ^+SR result with the prediction by first principles calculations for $Li_{7/8}MPO_4$ at ambient temperature.[16] It should be noted that the predicted D_{Li} (D_{Li}^{calc}) is mainly governed by the Li^+ jump between the occupied regular Li site and vacant regular Li site, while the μ^+SR results corresponds to the jump from the regular Li site to the interstitial site. Since such vacancies in the regular Li site are, in principle, known to increase D_{Li},[9] the discrepancy between D_{Li} and D_{Li}^{calc} would be acceptable for $LiFePO_4$ and $LiCoPO_4$.

However, it is very difficult to find a reasonable explanation for the discrepancy between D_{Li} and D_{Li}^{calc} for $LiNiPO_4$. If $D_{Li}^{calc} = 10^{-5}$ cm^2/s for $Li_{7/8}NiPO_4$, D_{Li} is most likely to range around 10^{-6} or 10^{-7} cm^2/s for $LiNiPO_4$, from the analogy with $LiFePO_4$ and $LiCoPO_4$ in Table IV. This means that ν should range between 10^{10} and 10^{11} s^{-1} for $LiNiPO_4$, which is too fast to explain the change in ν and Δ at 200 to 300 K [Figs. 4(a) and 4(b)] and the observation of a KT behavior [Figs. 2(g)–2(i)]. Furthermore, based on electrical conductivity measurements,[45] ionic conductivity (σ_{Li}) for $LiNiPO_4$ is comparable to or less than σ_{Li} for $LiMnPO_4$ and $LiCoPO_4$. This is in contrast to the prediction from the calculations, because σ_{Li} is proportional to D_{Li} for insulating materials. Furthermore, since $LiNiPO_4$ is known to lack a reversible Li deintercalation and intercalation reaction,[51,52] electrochemical measurements provide no crucial information on D_{Li} and/or $\tilde{D}_{Li}$.

Concerning E_a, the value for $LiFePO_4$ obtained by μ^+SR is about 1/5 of E_a along the b direction (540 ± 50 meV) estimated from ac impedance measurements for single-crystal $LiFePO_4$.[39] In addition, for polycrystalline $LiMPO_4$ with $M =$ Mn, Co, or Ni, E_a is reported to range between 0.61

TABLE IV. Magnitude of D_{Li} at 300 K and the activation energy (E_a) obtained by present μ^+SR measurements. D_{Li} at 300 K was estimated by extrapolation of the linear fit with E_a [see Fig. 8(b)]. The predicted values from first principles calculations (D_{Li}^{calc} and E_a^{calc}) for $Li_{7/8}MPO_4$[16] are also listed for comparison.

M	D_{Li} at 300 K (cm^2/s)	E_a (eV)	D_{Li}^{calc} (cm^2/s)	E_a^{calc} (meV)
Mn			10^{-9}	250
Fe	$3.6\,(2) \times 10^{-10}$	0.10 (2)	10^{-8}	270
Co	$1.6\,(1) \times 10^{-10}$	0.10 (1)	10^{-9}	360
Ni	$2.7\,(4) \times 10^{-10}$	0.17 (2)	10^{-5}	130

and 0.65 eV.[45] The discrepancy between E_a obtained by μ^+SR and ac impedance is due to the fact that μ^+SR is especially sensitive to short-range jumps of Li^+ ions, while ac impedance senses the long-range Li diffusion. In other words, since μ^+SR is a local probe, a powder sample is approximately equivalent to a single-crystal sample for muons. A very similar discrepancy between E_a obtained by NMR and ac impedance is also reported for several materials.[53]

V. SUMMARY

We have investigated the high-T diffusive behavior of LiMPO$_4$ with M = Mn, Fe, Co, or Ni by means of μ^+SR. Although it was difficult to measure the nuclear field relaxation in LiMnPO$_4$ due to large Mn^{2+} moments, a characteristic change in the nuclear field accompanied with Li^+ diffusion was observed for LiFePO$_4$, LiCoPO$_4$, and LiNiPO$_4$ above 150 K. By combining these results with the electrostatic potential calculations, the self-diffusion coefficients of Li ions at 300 K were estimated as $\sim 3.6\,(2) \times 10^{-10}$ cm^2/s for LiFePO$_4$, $\sim 1.6\,(1) \times 10^{-10}$ cm^2/s for LiCoPO$_4$, and $\sim 2.7\,(4) \times 10^{-10}$ cm^2/s for LiNiPO$_4$.

ACKNOWLEDGMENTS

We thank the staff of J-PARC and TRIUMF for help with the μ^+SR experiments. We also thank J. H. Brewer of the University of British Columbia for discussions. K. H. C. is supported by NSERC of Canada and (through TRIUMF) by NRC of Canada. A part of this work was supported by a Grant-in-Aid for Scientific Research on Innovative Areas "Ultra Slow Muon" (No. 23108003), of the Ministry of Education, Culture, Sports, Science, and Technology, Japan. All images involving crystal structure were made with VESTA.[54]

APPENDIX: FITTING THE SPECTRA

Here, we wish to show the reliability of the assumption that both λ_F and λ_{KT} are T independent. Figure 9 shows the T dependencies of the μ^+SR parameters, when we fit the ZF and LF spectra using a common A_{BG} in the whole T range and H_{LF}-independent Δ and ν at each T using Eq. (1). Such an individual fit result, particularly ν, is compared with the global fit result for LiFePO$_4$ and LiCoPO$_4$.

According to the structural analysis of LiFePO$_4$ made using synchrotron radiation x-ray diffraction data,[13] there is no structural variation in the FeO$_6$ octahedron in the T range between 100 and 450 K. This suggests that the contribution of the electronic field does not alter with T or might vary with $1/T$ accompanied with the $\chi(T)$ curve (Fig. 1). In fact, the $\lambda_F(T)$ curve for LiFePO$_4$ is found to lack a systematic T dependence. On the contrary, the $\lambda_{KT}(T)$ curve is similar to the $\Delta(T)$ curve, while the magnitude of λ_{KT} is about 1/5 of Δ. Such a T dependence of λ_{KT} should be attributed to that of Δ or ν, since λ_{KT} also comes from the contribution of the electronic field. Therefore, it is reasonable to assume that both λ_F and λ_{KT} are T independent in the T range between 100 and 500 K for LiFePO$_4$.

For LiCoPO$_4$, χ measurements and both x-ray and neutron diffraction studies revealed the absence of a structural phase transition below ambient T.[31,32,55] This is also confirmed

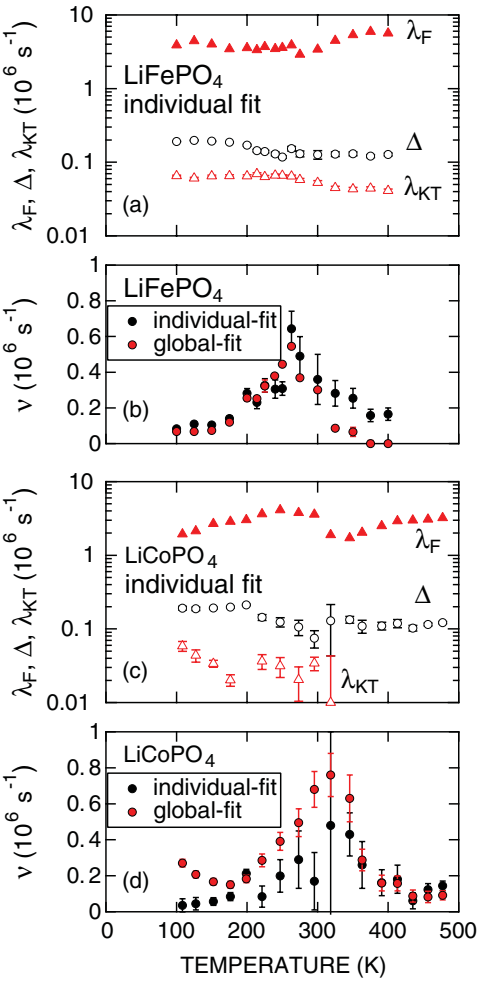

FIG. 9. (Color online) T dependencies of the μ^+SR parameters obtained by an *individual fit*; (a) λ_F, Δ, and λ_{KT} for LiFePO$_4$, (b) ν for LiFePO$_4$, (c) λ_F, Δ, and λ_{KT} for LiCoPO$_4$, and (d) ν for LiCoPO$_4$. In (b) and (d), the data for ν estimated by a *global fit* are also plotted for comparison.

by the $\chi(T)$ curve for the present sample below 400 K (Fig. 1). Hence, both λ_F and λ_{KT} are expected to be T independent for LiCoPO$_4$. Indeed, the T dependence of λ_F for LiCoPO$_4$ is similar to that for LiFePO$_4$, whereas λ_F(LiCoPO$_4$) $< \lambda_F$(LiFePO$_4$), as expected from Table II and Fig. 6. In addition, λ_{KT} is likely to be almost independent of T below 300 K, while λ_{KT} becomes too small to be detected above 300 K. Consequently, the most acceptable scenario is that both λ_F and λ_{KT} are also T independent for LiCoPO$_4$, as in the case for LiFePO$_4$.

In other words, the T dependencies of λ_F and λ_{KT} are caused by an artificial effect of the fitting; that is, the nuclear field contribution is not perfectly separated by the electronic field contribution, even by a combination of ZF and LF measurements, if we use an individual fit at each T. Nevertheless, although such an individual fit alters ν, the overall nature of the $\nu(T)$ curve obtained by an individual fit are essentially the same as that obtained by a global fit for both compounds [Figs. 9(b) and 9(d)]. This is also supported by the LiNiPO$_4$ results, for which both λ_F and λ_{KT} are negligibly small.

*e0589@mosk.tytlabs.co.jp
†Present address: Comprehensive Research Organization for Science and Society (CROSS), 162-1 Shirakata, Tokai, Ibaraki 319-1106, Japan.

[1]G. M. Kalvius, D. R. Noakes, and O. Hartmann, *Handbook on the Physics and Chemistry of Rare Earths*, edited by K. A. Gschneidner Jr., L. Eyring, and G. H. Lander (North-Holland, Amsterdam, 2001), Vol. 32, Chap. 206.
[2]T. Matsuzaki, K. Nishiyama, K. Nagamine, T. Yamazaki, M. Senba, J. M. Bailey, and J. H. Brewer, Phys. Lett. A **123**, 91 (1989).
[3]R. S. Hayano, Y. J. Uemura, J. Imazato, N. Nishida, T. Yamazaki, and R. Kubo, Phys. Rev. B **20**, 850 (1979).
[4]J. Sugiyama, K. Mukai, Y. Ikedo, H. Nozaki, M. Månsson, and I. Watanabe, Phys. Rev. Lett. **103**, 147601 (2009).
[5]K. Mizushima, P. C. Jones, P. J. Wiseman, and J. B. Goodenough, Mater. Res. Bull. **15**, 783 (1980).
[6]I. Tomeno and M. Oguchi, J. Phys. Soc. Jpn. **67**, 318 (1998).
[7]K. Nakamura, M. Yamamoto, K. Okamura, Y. Michihiro, I. Nakabayashi, and T. Kanashiro, Solid State Ionics **121**, 301 (1999).
[8]K. Nakamura, H. Ohno, K. Okamura, Y. Michihiro, I. Nakabayashi, and T. Kanashiro, Solid State Ionics **135**, 143 (2000).
[9]A. Van der Ven and G. Ceder, Electrochem. Solid-State Lett. **3**, 301 (2000).
[10]J. Sugiyama, Y. Ikedo, K. Mukai, H. Nozaki, M. Månsson, O. Ofer, M. Harada, K. Kamazawa, Y. Miyake, J. H. Brewer, E. J. Ansaldo, K. H. Chow, I. Watanabe, and T. Ohzuku, Phys. Rev. B **82**, 224412 (2010).
[11]A. K. Padhi, K. S. Nanjundaswamy, and J. B. Goodenough, J. Electrochem. Soc. **144**, 1188 (1997).
[12]W.-J. Zhang, J. Power Sources **196**, 2962 (2011), and references cited therein.
[13]J. Sugiyama, H. Nozaki, M. Harada, K. Kamazawa, O. Ofer, M. Månsson, J. H. Brewer, E. J. Ansaldo, K. H. Chow, Y. Ikedo, Y. Miyake, K. Ohishi, I. Watanabe, G. Kobayashi, and R. Kanno, Phys. Rev. B **84**, 054430 (2011).
[14]P. J. Baker, I. Franke, F. L. Pratt, T. Lancaster, D. Prabhakaran, W. Hayes, and S. J. Blundell, Phys. Rev. B **84**, 174403 (2011).
[15]A. V. Churikov, A. V. Ivanishchev, I. A. Ivanishcheva, V. O. Sycheva, N. R. Khasanova, and E. V. Antipov, Electrochim. Acta **55**, 2939 (2010).
[16]D. Morgan, A. Van der Ven, and G. Ceder, Electrochem. Solid-State Lett. **7**, A30 (2004).
[17]P. P. Prosini, M. Lisi, D. Zane, and M. Pasquali, Solid State Ionics **148**, 45 (2002).
[18]D. Y. W. Yu, C. Fietzek, W. Weydanz, K. Donoue, T. Inoue, H. Kurokawa, and S. Fujitani, J. Electrochem. Soc. **154**, A253 (2007).
[19]P. He, X. Zhang, Y.-G. Wang, L. Cheng, and Y.-Y. Xia, J. Electrochem. Soc. **155**, A144 (2008).
[20]X.-C. Tang, L.-X. Li, Q.-L. Lai, X.-W. Song, and L.-H. Jiang, Electrochim. Acta **54**, 2329 (2009).
[21]J. Ma, B. Li, H. Du, C. Xu, and F. Kang, J. Electrochem. Soc. **158**, A26 (2011).
[22]C. M. Julien, A. Ait-Salah, A. Mauger, and F. Gendron, Inoics **12**, 21 (2006).
[23]D. Arcon, A. Zorko, R. Dominko, and Z. Jagličič, J. Phys. Condens. Matter **16**, 5531 (2004).
[24]M. Kopec, A. Yamada, G. Kobayashi, S. Nishimura, R. Kanno, A. Mauger, F. Gendron, and C. M. Julien, J. Power Sources **189**, 1154 (2009).
[25]R. P. Santoro and R. E. Newnham, Acta Crystallogr. **22**, 344 (1967).
[26]G. Rousse, J. Rodriguez-Carvajal, S. Patoux, and C. Masquelier, Chem. Mater. **15**, 4082 (2003).
[27]G. Liang, K. Park, J. Li, R. E. Benson, D. Vaknin, J. T. Markert, and M. C. Croft, Phys. Rev. B **77**, 064414 (2008).
[28]J. Li, V. O. Garlea, J. L. Zarestky, and D. Vaknin, Phys. Rev. B **73**, 024410 (2006).
[29]J. M. Mays, Phys. Rev. **131**, 38 (1963).
[30]J. Li, W. Tian, Y. Chen, J. L. Zarestky, J. W. Lynn, and D. Vaknin, Phys. Rev. B **79**, 144410 (2009).
[31]R. P. Santoro, D. J. Segal, and R. E. Newnham, J. Phys. Chem. Solids **27**, 1192 (1966).
[32]D. Vaknin, J. L. Zarestky, L. L. Miller, J.-P. Rivera, and H. Schmid, Phys. Rev. B **65**, 224414 (2002).
[33]W. Tian, J. Li, J. W. Lynn, J. L. Zarestky, and D. Vaknin, Phys. Rev. B **78**, 184429 (2008).
[34]D. Vaknin, J. L. Zarestky, J.-P. Rivera, and H. Schmid, Phys. Rev. Lett. **92**, 207201 (2004).
[35]T. B. S. Jensen, N. B. Christensen, M. Kenzelmann, H. M. Ronnow, C. Niedermayer, N. H. Andersen, K. Lefmann, J. Schefer, M. v. Zimmermann, J. Li, J. L. Zarestky, and D. Vaknin, Phys. Rev. B **79**, 092412 (2009).
[36]O. Ofer, J. Sugiyama, J. H. Brewer, M. Månsson, K. Prša, E. J. Ansaldo, G. Kobayashi, and R. Kanno, in *Abstract Book of 12th International Conference on Muon Spin Rotation, Relaxation, and Resonance (μSR2011)* (Physics Procedia, in press), p. 53.
[37]W. Higemoto, T. U. Ito, K. Ninomiya, R. H. Heffner, K. Shimomura, K. Nishiyama, and Y. Miyake, J. Phys.: Conf. Ser. **225**, 012012 (2010).
[38]S. Nishimura, G. Kobayashi, K. Ohoyama, R. Kanno, M. Yashima, and A. Yamada, Nat. Mater. **7**, 707 (2008).
[39]J. Li, W. Yao, S. Martin, and D. Vaknin, Solid State Ionics **179**, 2016 (2008).
[40]R. Akiyama, Y. Ikedo, M. Månsson, T. Goko, J. Sugiyama, D. Andreica, A. Amato, K. Matan, and T. J. Sato, Phys. Rev. B **81**, 024404 (2010).
[41]J. Sugiyama (unpublished).
[42]C. T. Kaiser, V. W. J. Verhoeven, P. C. M. Gubbens, F. M. Mulder, I. de Schepper, A. Yaouanc, P. Dalmas de Réotier, S. P. Cottrell, E. M. Kelder, and J. Schoonman, Phys. Rev. B **62**, R9236 (2000).
[43]M. J. Ariza, D. J. Jones, J. Roziére, J. S. Lord, and D. Ravot, J. Phys. Chem. B **107**, 6003 (2003).
[44]J. Sugiyama, K. Mukai, Y. Ikedo, P. L. Russo, T. Suzuki, I. Watanabe, J. H. Brewer, E. J. Ansaldo, K. H. Chow, K. Ariyoshi, and T. Ohzuku, Phys. Rev. B **75**, 174424 (2007).
[45]K. Rissouli, K. Benkhouja, J. R. Ramos-Barrado, and C. Julien, Mater. Sci. Eng. B **98**, 185 (2003).
[46]K. M. Kojima, J. Yamanobe, H. Eisaki, S. Uchida, Y. Fudamoto, I. M. Gat, M. I. Larkin, A. Savici, Y. J. Uemura, P. P. Kyriakou, M. T. Rovers, and G. M. Luke, Phys. Rev. B **70**, 094402 (2004).
[47]R. J. Borg and G. J. Dienes, in *An Introduction to Solid State Diffusion* (Academic Press, San Diego, 1988).
[48]Y. Wang, Y. Yang, Y. Yang, and H. Shao, Solid State Commun. **150**, 81 (2010).

[49]J.-W. Lee, M.-S. Park, B. Anass, J.-H. Park, M.-S. Paik, and S.-G. Doo, Electrochim. Acta **55**, 4162 (2010).
[50]A. Eftekhari, J. Electrochem. Soc. **151**, A1456 (2004).
[51]S. Okada, S. Sawa, M. Egashira, J. I. Yamaki, M. Tabuchi, H. Kageyama, T. Konishi, and A. Yoshino, J. Power Sources **97-98**, 430 (2001).
[52]J. Wolfenstine and J. Allen, J. Power Sources **136**, 150 (2004).
[53]P. Heitjans and S. Indris, J. Phys. Condens. Matter **15**, R1257 (2003).
[54]K. Momma and F. Izumi, J. Appl. Cryst. **41**, 653 (2008).
[55]H. Ehrenberg, N. N. Bramnik, A. Senyshyn, and H. Fuess, Solid State Sci. **11**, 18 (2009).